ADENINE INTERACTION WITH AND ADSORPTION ON Fe-ZSM-5 ZEOLITES: A PREBIOTIC CHEMISTRY STUDY USING DIFFERENT TECHNIQUES

Short Title: Interaction between adenine and Fe-ZSM-5 zeolites

Pedro R. Anizelli[1], João Paulo T. Baú[1], Daniel F. Valezi[2], Leila C. Canton[3], Cristine E. A. Carneiro[1], Eduardo Di Mauro[2], Antonio C. S. da Costa[3], Douglas Galante[4], Adriano H. Braga[5], Fabio Rodrigues[6], Joaquín Coronas[7], Clara Casado-Coterillo[8], Cássia T B. V. Zaia[9] and Dimas A. M. Zaia[1*]

[1]Laboratório de Química Prebiótica, Departamento de Química-CCE, [2]Departamento de Física-CCE, Universidade Estadual de Londrina, 86051-990, Londrina-PR, Brazil; [3]Departamento de Agronomia-CCA, Universidade Estadual de Maringa, 87020-900, Maringá-PR, Brazil; [4]Laboratório Nacional de Luz Síncrotron, 13083-100, Campinas-SP, Brazil; [5]Departamentp de Engenharia Química 13565905, São Carlos-SP, Brazil; [6]Instituto de Química, Universidade de São Paulo, 05508-000, São Paulo-SP, Brazil; [7]Chemical and Environmental Engineering Department and Nanoscience Institute of Aragon, Universidad de Zaragoza, 50009, Zaragoza, Spain; [8]Depatment of Chemical & Biomolecular Engineering, Universidad de Cantabria, 39005, Santander, Spain. [9]Departamento de Ciências Fisiológicas-CCB, Universidade Estadual de Londrina, 86051-990, Londrina-PR, Brazil

*Corresponding author: Dr. Dimas A. M. Zaia
Departamento de Química-CCE
Universidade Estadual de Londrina
86051-990, Londrina-PR, Brazil
e-mail: damzaia@uel.br; dimaszaia.quimicaprebiotica@gmail.com
Phone:55-43-3371-4366
Fax: 55-43-3371-4286

Abstract

Most adsorption experiments are performed under conditions that did not exist on Earth before the life arose on it. Because adsorption is the first step for all other processes (protection against degradation and polymerization), it is important that it is performed under conditions that existed on prebiotic Earth. In this paper, we use an artificial seawater (seawater 4.0 Ga), which contains major cations and anions that could present on the oceans of the prebiotic Earth. In addition, zeolites, with substituted Fe in the framework, and adenine were probably common substances on the prebiotic Earth. Thus, study the interaction between them is an important issue in prebiotic chemistry. There are two main findings described in this paper. Firstly, zeolites with different Si/Fe ratios adsorbed adenine differently. Secondly, XAFS showed that, after treatments with seawater 4.0 Ga and adenine, an increase in the complexity of the system occurred. In general, salts of seawater 4.0 Ga did not affect the adsorption of adenine onto zeolites and adenine adsorbed less onto zeolites with iron isomorphically substituted. The C=C and NH_2 groups of adenine interacted with the zeolites. Gypsum, formed from aqueous species dissolved in seawater 4.0 Ga, precipitated onto zeolites. EPR spectra of zeolites showed lines caused by Fe framework and Fe^{3+} species. TG curves of zeolites showed events caused by loss of water weakly bound to zeolite (in the 30 - 140 °C range), water bounded to iron species or cations from seawater 4.0 Ga or located in the cavities of zeolites (157 - 268 °C) and degradation of adenine adsorbed onto zeolites (360 - 600 °C). Mass loss follows almost the same order as the amount of adenine adsorbed onto zeolites. The XAFS spectrum showed that Fe^{3+} could be substituted into the framework of the Fe_7-ZSM-5 zeolite.

Keywords: prebiotic chemistry; adsorption; nucleic acid base; iron zeolites; seawater

1. INTRODUCTION

Zeolites are crystalline microporous aluminosilicates with a periodic arrangement of cages and channels and are widely distributed on the Earth [1, 2]. Zeolites are among the oldest minerals occurring on our planet [1, 3], and occur in several different geologic environments including hydrothermal systems, sedimentary rocks, alkaline igneous rocks, and in miscellaneous joints and cavities in rocks [4-6].

Zeolites play important roles in several human activities and are used in adsorption and catalysis processes, agriculture, nuclear waste and fallout treatment, construction, and water and wastewater treatments [6-12]. Synthetic zeolites with Fe^{3+} incorporated into their framework have shown a catalytic effect for chemical reactions, degradation of dyes, and adsorption of salts [13-20].

Zeolites could also have played important roles in the origin of life on Earth by concentrating biomolecules and protecting them from degradation by UV radiation and hydrolysis, forming biopolymers and primitive cells [21-26]. In fact, relatively high silica zeolites such as mutinaite [27] and tschernichite [28], natural analogues of ZSM-5 and zeolite beta, respectively may have played a role in the biochemical evolution that occurred in the early history of Earth with the incorporation of amino acids into the first primitive proteins [28].

An important property of zeolites is their organophilic character, meaning that, unlike most minerals, they can adsorb uncharged biomolecules as much as they can adsorb charged biomolecules [24, 29, 30]. The hydrophilic/hydrophobic character of zeolites can be modified by changing the Si/Al ratio or the metal in the crystalline framework. The isomorphic substitution

of Si by trivalent cations such as B^{+3}, Al^{+3} and Fe^{+3} create more Bronsted acid sites in the zeolite [31]. Because iron is the fourth most abundant element in the crust of Earth, it should be expected to be incorporated in the framework of natural zeolites [32-34].

Nucleic acid bases were probably synthesized on the prebiotic Earth and were also delivered by exogenous sources such as meteorites, comets, or interplanetary dust particles. Adenine (Figure 1), which is used in this work, was found in meteorites and formed under conditions found on the prebiotic Earth [35-38].

In addition, there is evidence for the existence of liquid water on Earth 4.4 billion years ago [39], the first permanent ocean was probably formed 3.9 billion year ago, after a decrease in heavy bombardment [40]. According to Knauth [41] the primitive oceans were 1.5 to 2 times more saline than today and Na^{+} and Cl^{-} were not the major ions. Using the work of Izawa et al. [42], Zaia [30] suggested an artificial seawater in which the major ions are Mg^{2+}, Ca^{2+} and SO_4^{2-}. This seawater, probably, resembles more closely (than modern-day seawater) the real composition of seawater of the prebiotic Earth and is hereafter, in this work, referred to as Seawater 4.0 Ga. As suggested by Zaia [30], studies of adsorption of biomolecules onto minerals, as well as prebiotic chemical reactions, should be performed in artificial seawater solutions that resemble the ancient oceans rather than in solutions of ultrapure water or NaCl. Using a seawater that more closely resembles the oceans of the prebiotic Earth in terms of its major cations and anions is of paramount importance for experiments in prebiotic chemistry because interactions between the cations and anions from the seawater and the organic molecules and

minerals can alter the adsorption process [3, 20, 29, 30]. Seawater 4.0 Ga better resembles the chemical composition of primitive oceans, meaning that the results obtained will be more reliable than those of experiments performed in ultrapure water or saline solutions.

Because both adenine and zeolites, including Fe-zeolites, were present in the prebiotic Earth, the interaction among them is an important issue for understanding prebiotic chemistry. In the present work the adsorption of adenine (Figure 1) onto Fe_{ext}-ZSM-5 (material with Fe^{3+} exchangeable) and Fe-ZSM-5 zeolites was studied at pH 4.0 both in ultrapure water and in a seawater solution with a chemical composition that resembles the major cations and anions of the seawater of 4.0 billion years ago (4.0 Ga). FTIR spectroscopy, thermal analysis, scanning electron microscopy (SEM), electronic paramagnetic resonance (EPR), X-ray diffraction, and Fe K-edge XAFS methods were used to study the interactions between adenine and zeolites.

2. MATERIALS AND METHODS

2.1. Materials

2.1.1. Adenine and ZSM-5 zeolite

Adenine (Figure 1) was purchased from Sigma Aldrich and was used as received. Commercial ZSM-5 zeolite with Si/Al = 25 was supplied by Zeolyst International.

2.1.2. Synthesis of Fe_{ext}-ZSM-5 and Fe-ZSM-5 zeolites

Fe_{ext}-ZSM-5 was prepared by wet ion exchange (WIE) according to the procedure reported by Melián-Cabrera et al. [43] on the as received ZSM-5

sample by stirring 1.446 g of the parent zeolite in a 2.0 wt % Fe^{3+} solution at initial pH 2.5, at room temperature for 2 h.

Fe-zeolites (Fe_3-ZSM-5, Fe_4-ZSM-5, Fe_5-ZSM-5, Fe_6-ZSM-5, and Fe_7-ZSM-5) were prepared using a methodology adapted from Tuan et al. [31] for isomorphously substituted ZSM-5-based membranes. The gel was prepared from a mixture of silica sol (Ludox AS40) as silicon source and tetrapropylammonium hydroxide (TPAOH) as a structure-directing agent, for later addition of iron nitrate ($Fe(NO_3)_3$). The composition of the gel was 1.5 TPAOH 19.5 SiO_2:0.195Fe^{3+}:438 H_2O with a Si/Fe ratio of 100 for all samples. Volume gel, temperature, and agitation time for gel formation were varied (Table 1). The gel was added in the autoclave for hydrothermal synthesis. The temperature of the autoclave was maintained at 185°C for all samples. As measured by energy dispersive X-ray (EDX), the Si/Fe ratios in the samples ranged from 4.6 to 18 (Tables 1, 2). The amount of each zeolite obtained is shown in Table 1.

2.1.3. Seawater 4.0 Ga

The following substances were weighed and dissolved in 1.0 L of solution with ultrapure water: 1.909 x 10^{-3} mol of sodium sulfate, 2.457 x 10^{-3} mol of magnesium chloride hexahydrate, 1.701 x 10^{-2} mol of calcium chloride dihydrate, 4.730 x 10^{-4} mol of magnesium bromide, 2.296 x 10^{-2} mol of potassium sulfate, and 0.1242 mol of magnesium sulfate [30].

2.2. Methods

2.2.1. Adsorption of adenine

Adenine was dissolved in ultrapure water and seawater 4.0 Ga at a concentration of 720 μg mL^{-1}. The zeolite (20 mg, either Fe_{ext}-ZSM-5 or Fe-ZSM-5 zeolite) was placed in an Eppendorf tube (1.5 mL) containing: (a) 1.0 mL of seawater 4.0 Ga with or without 720 μg mL^{-1} of adenine or (b) 1.0 mL of

ultrapure water with or without 720 μg mL^{-1} of adenine. For standardization, the pH of the solutions was adjusted to 4.0 by adding 1.0 mol L^{-1} HCl and stirring for 24 h at room temperature before being centrifuged for 10 minutes at 6000 rpm. The solid was separated from the supernatant, lyophilized, and analyzed using FTIR, thermal analyses (TG), scanning electron microscopy (SEM), X-ray diffractometry, electronic paramagnetic resonance (EPR) and XAFS. After it was lyophilized, the supernatant was used for nucleic acid measurements (see below) and analyzed by electronic paramagnetic resonance (EPR).

2.2.2. UV/VIS spectrophotometric method

Absorbance was determined using a Shimadzu UV–Vis spectrophotometer. Adenine was determined by reading the absorbance in the UV region using a wavelength of 260 nm. The following equation was used for the calculation of the amount of base adsorbed on the zeolite:

$C_{adsorbed\ (\mu g)} = (C_{initial} - C_{solution})$, where $C_{solution} = [\ (C_{initial})\ (Abs_{sample}/Abs_{initial})]$.

2.2.3. FTIR spectroscopy

The IR spectra were recorded with a Shimadzu 8300 FTIR spectrophotometer. KBr disc pellets were prepared and spectra were recorded in transmission mode from 400 cm^{-1} to 4000 cm^{-1} with a resolution of 4 cm^{-1} and 98 accumulations. FTIR spectra were analyzed using the Origin software (Origin Lab Corporation, version 8.0, 2007).

2.2.4. Electronic paramagnetic resonance (EPR) spectroscopy

The samples were analyzed by EPR at X-band (ca. 9.5 GHz) with a 20 G modulation amplitude and magnetic field modulation of 100 kHz using a JEOL

(JES-PE- 3X) spectrometer at room temperature. 2,2-diphenyl-1-picrylhydrazyl (DPPH) was used as the g-marker and standard for line intensity, using its two spectral lines. The g-factor (g_2) of each line in the EPR spectra was calculated using the equation:

$$g_2 = \frac{g_1 B_1}{B_2} \quad \textbf{(1)}$$

where g_1 is the value of the DPPH g-factor (g=2.004) and B_1 and B_2 are the magnetic field values of the central line of DPPH and sample, respectively.

2.2.5. X-Ray diffractometry

Zeolites were analyzed by powder X-ray diffraction using a Shimadzu D 6000 diffractometer using Co Kα radiation (40 kV, 30 mA) and an iron filter in a step-scanning mode (0.02°2θ/0.6 s). All peak positions were analyzed using Grams software (Thermo Scientific, version 8.0).

2.2.6. Thermal Analyses (TG)

The TG curves of lyophilized samples were obtained with a Perkin-Elmer TGA 4000, with a scan from 50 °C to 900 °C, with a heating ratio of 10 °C/min, a nitrogen flow of 20 mL/min, and using 20 mg of sample.

2.2.7. Scanning Electron Microscopy (SEM)

The morphology of Fe-zeolite particles was observed using a HITACHI S2300 scanning electron microscope at 10 kV on gold sputtered samples.

2.2.8. BET isotherm

A Micromeritics Tristar 3000 was used to obtain the N_2 adsorption isotherm and calculate the Brunauer, Emmett, and Teller (BET) specific surface

area. The BET surface area was determined from a plot of $P/v(P_0-P)$ versus P/P_{A0} from equation:

$$\frac{P}{v(P_o-P)} = \frac{1}{v_m.C} + \frac{(c-1)P}{C.v_m.P_0} \quad \textbf{(2)}$$

where P_0 is the equilibrium pressure, P is the saturation pressure, v is the adsorbed gas volume, v_m is the monolayer adsorbed gas volume, and C is a BET constant. The surface areas and pore sizes of all zeolites are summarized in table 1. Samples were degassed at 200 °C for 8 h under vacuum before measurement.

2.2.9. XAFS data collection

X-ray absorption spectra of the Fe K-edge were collected at the XAFS1 beamline of, LNLS – Brazilian Synchrotron Light Laboratory (under proposal XAFS1-16161). The energy was calibrated for each scan by the Fe K-edge of an iron foil. The samples were prepared as disc pellets and supported on slides with Kapton tap.

2.2.10. XAFS data processing

The XAFS fits were performed using k^1, k^2 and k^3 weighting. The reference material used was Fe_2O_3 (hematite) for Fe-O and Fe-Fe, according to parameters reported by Blake et al [44]. The softwares Athena and Artemis were used for data processing. The ATOMS and FEFF6 computer codes were used for ab initio calculations.

2.2.11. Statistical Analysis

The Tukey test was used to compare means at a significance level of $p < 0.05$.

3. RESULTS AND DISCUSSION

3.1. Adsorption

Table 2 shows the amount of adenine adsorbed onto Fe_{ext}-ZSM-5 and Fe-ZSM-5 zeolites at pH 4.00 in two different solvents (ultrapure water and seawater 4.0 Ga). The adsorption order of adenine onto zeolites, in ultrapure water and seawater 4.0 Ga, were: $Fe_{ext} > Fe_7 > Fe_4 > Fe_5 = Fe_3 > Fe_6$ and $Fe_{ext} > Fe_7 > Fe_4 > Fe_5 > Fe_3 > Fe_6$, respectively (Table 2; $p < 0.05$). Using Seawater 4.0 Ga, the amount of adenine adsorbed onto Fe_{ext}-ZSM-5 was 33.1 μg mg^{-1}. Using a different artificial seawater, Baú et al. [25] obtained a similar amount (27.4 μg mg^{-1}) of adenine adsorbed onto ZSM-5. Because zeolites have a permanent negative charge [45] and the pKa of adenine is 4.20, it is positively charged at pH < 4.20 due to the protonation of nitrogen 1 (Figure 1) [46], the interaction between them could be electrostatic which explains the similar adsorption even though the adenine was dissolved in different seawaters. Electrostatic interactions were also cited as an explanation for the interaction between adenine and clay minerals at acidic pH [47-52]. Studies of the adsorption of nitrogenous base onto TiO_2 show that this material has a higher adsorption capacity at pH < 5.00 for adenine and cytosine than other nitrogenous bases [53]. Adenine adsorption onto clays was also higher than that of uracil and thymine [54]. Another study of adenine adsorption on different materials observed the adsorption order: pyrite > quartz > pyrrhotite > forsterite > magnetite. The authors attributed this difference to the difference between the mineral crystal structures and the relative proportions of uncharged surface sites [55]. Compared with the seawater used by Baú et al. [25], Benetoli et al. [50], and Carneiro et al. [52], which is rich in Na^+ and Cl^-, the seawater used in this paper better resembles the oceans of the prebiotic Earth, with high concentrations of Mg^{2+}, Ca^{2+}, and SO_4^{2-}; thus, the results are more significant.

Seawater 4.0 Ga had an effect on the adsorption of adenine for the Fe_7-ZSM-5 zeolite, with higher values in ultrapure water (Table 2, $p < 0.05$). A similar result was observed by Winter and Zubay [48] when adenine was adsorbed onto montmorillonite in artificial seawater rather than in a buffer solution. For other zeolites the adsorption was similar in both solvents (Table 2, $p > 0.05$). This is a positive result, because if the adsorption did not occur all other roles played by minerals could be compromised. Thus, in prebiotic studies, is important to use a seawater whose chemical composition resembles that of the oceans of primitive Earth.

For Fe-ZSM-5 zeolites, the amount of adenine adsorbed is significantly lower than it is for Fe_{ext}-ZSM-5 and this effect can be a result of the presence of iron in the structure of material. Because, in the synthesis of zeolites, iron replaces the silicon, in general, the increase of Si/Fe ratio decreases the amount of adenine adsorbed (Table 2, $p < 0.05$), since the material has a lower negative charge and the electrostatic interaction is diminished. However, the Fe_7-ZSM-5 has the highest value of Si/Fe ratio, but this material showed the highest adsorption among Fe-ZSM-5 zeolites (Table 2). One explanation for this observation is that the Fe_7-ZSM-5 zeolite has the largest pore volume, probably due to the generation of some mesoporosity, during the synthesis (in agreement with the SEM characterization shown below), enabling higher adsorption than other zeolites with iron isomorphically substituted (Table 2). The pore volume is an important parameter that directly influences the adsorption. Adsorption experiments for amino acids on ZSM-5 and ZSM-11 showed a selective adsorption of leucine in the presence of phenylalanine because the lower pore volume of these materials favored the diffusion of smaller molecules like leucine

over phenylalanine [56]. Gonzalez-Olmos et al. [16] observed that the adsorption of MTBE (methyl tert-butyl ether) was higher in Fe-beta zeolite than on Fe-ZSM-5 zeolite because of the difference in pore volume for these materials. Because the Fe-beta zeolite has larger pore dimensions (6.5 Å x 5.6 Å and 7.5 Å x 5.7 Å) than Fe-ZSM-5 zeolite (5.1 Å x 5.5 Å and 5.4 Å x 5.6 Å) and the MTBE has a diameter of 6.2 Å, the molecule should be more easily able to enter the pores of the beta zeolite. In addition, as in case of Al-ZSM-5 zeolites, the higher Si/Fe ratio the lower the hydrophilicity (due to minor content in exchanging sites), favoring the adsorption of organic compounds over that of water. Other explanation for the higher adsorption observed in Fe_7-ZSM-5 zeolite is the smaller particle aggregation observed for this material in SEM images (Figure 3). Small particles provide higher contact surface for the adsorption of adenine onto Fe_7-ZSM-5 zeolite. As shown in Figure 3 others Fe-ZSM-5 zeolites have higher aggregation levels and particle size. Gorshunova et al [57] suggested that the zeolite size affect the rate of diffusion of adsorbate molecules into material surface. The adsorption rate in mordenite with higher particle size is somewhat less than mordenite with lower particle size [57].

The infrared spectrum of adenine (Figure 2 a_1, b_1) in the region between 1550 $cm^{-1}$and 1750 cm^{-1} showed two bands at 1603 cm^{-1} and 1673 cm^{-1}, which can be attributed to C=C stretching and NH_2 in plane bending, respectively [26, 58, 59]. In the same region, Fe_{ext}-ZSM-5 and Fe_7-ZSM-5 showed a band at 1631cm^{-1} (Figure 2 a_4, b_4), attributed to the bending of O-H groups in the hydration water of the mineral [25, 60]. The spectra a_2 and a_3 of figure 2 are for lyophilized samples of Fe_{ext}-ZSM-5 after adsorption of adenine in ultrapure water and seawater 4.0 Ga, respectively, at pH 4.00. The spectra showed that

the band at 1603 cm^{-1} was shifted to1626 cm^{-1} and the band at 1673 cm^{-1} was shifted to 1694 cm^{-1}. These data suggest that the site for the interaction of the adenine with the mineral is the C=C group from the six-membered ring of adenine and the NH_2 group. However, the band at 1626 cm^{-1} was in the same region as the bending of the O-H group of the hydration water from the zeolite. The same behavior occurs in the Fe_7-ZSM-5 zeolite after adsorption of adenine onto the zeolite (Figure 2, b_2, b_3). Another possibility is the formation of a complex between the cations Ca^{2+} and Mg^{2+} from the artificial seawaters, adsorbed onto zeolites and adenine [26]. The chelation occurs in the bidentate position through the NH_2 group and nitrogen of the imidazole ring [26]. This result shows that is important to have a seawater whose composition resembles the composition of the oceans of primitive Earth, because the salts affect the adsorption process. Protonated adenine has bands at 1573 cm^{-1}, 1609 cm^{-1} and 1699 cm^{-1} [26]. The pH 4.0 is lower than pKa 1 of the nuclei acid base [46], and these bands are expected in the region 1550 cm^{-1} to 1750 cm^{-1}.However, the band at 1573 cm^{-1} was not observed in our spectra (Figure 2, a_2, a_3, b_2, b_3). Probably, deprotonation occurred when the adenine was adsorbed onto zeolites.

The NH_2 group could be also involved in the interaction of adenine with clays, zeolites, and metals [25, 50, 52, 61, 62]. However, McNutt et al. [63] suggested that the interaction between adenine and Cu (110) occurred through the N atoms from the pyrimidine ring. It should be noted that zeolites and clays are very different from Cu.

3.2. Interaction between adenine and zeolites

The Fe_{ext}-ZSM-5 and Fe-ZSM-5 zeolites were characterized using scanning electron microscopy (SEM), X-ray diffraction (XRD), electronic paramagnetic resonance (EPR), thermal analyses and XAFS. The images from the SEM showed that the commercial ZSM-5 particles were lower than 1 µm size (Figure 3 a). The isomorphic substitution of aluminum by iron did not change the morphology of the material, but the ZSM-5 crystals were assembled in spheres (Figure 3 b-e). However, these materials showed larger particle sizes as can be observed in Figure 3. Fe_{ext}-ZSM-5 (material with exchangeable Fe^{3+}) showed similar particles sizes to ZSM-5 precursor shown in Figure 3 a. However, Fe_7-ZSM-5 zeolite (Figure 3 f) presents a different morphology with nanosized particles (~ 100 nm) responsible for the especial adsorption properties above mentioned.

X-ray diffractograms show that stirring zeolites with ultrapure water and seawater 4.0 Ga, with and without adenine, and at pH 4.0 did not cause apparent dissolution of the minerals (Figure 4). This is an important result for prebiotic chemistry because the interaction between them likely involved adsorption [30]. It should be noted that adsorption is the first step for all other processes (protection against degradation, formation of polymers) that minerals may be involved in. In treatments using seawater 4.0 Ga, the diffractograms show one basal plane at 13.5 degrees that could be the result of the precipitation of gypsum ($CaSO_4$ $2H_2O$) onto the zeolites. These results are expected because seawater 4.0 Ga is rich in calcium and sulfate. Baú et al. [25] obtained similar results with synthetic zeolites mixed with artificial seawater. Finally, XRD did not show the presence of other peaks different from those corresponding to MFI-type zeolite structure of Fe-ZSM-5. This suggest no

detectable by XRD Fe present in the form of oxides, salts or crystalline complex species. As shown below, complementary characterization tools were need to address this important point.

EPR spectroscopy provides valuable information about the different symmetries or distortions resulting from substitution of the iron in Fe-ZSM-5 zeolites. Fe_4, Fe_6 and Fe_7-ZSM-5 zeolites showed three lines—two in the region at g ≈ 2 and another at g ≈ 4.7 (Figure 5). Fe_5-ZSM-5 showed two lines—one at g ≈ 2 and another at g ≈ 4.7 and Fe_{ext}-ZSM-5 showed one at g ≈ 2 (Figure 5). The lines at g ≈ 2 could be a result of Fe_xO_y clusters and Fe^{3+} framework species [14, 15]. As pointed out by Fejes et al. [14], Fe^{3+} can be incorporated into the zeolite as a framework or extra-framework component and iron hydroxide (FeO·(OH), $Fe(OH)_3$) and iron oxide clusters that do not interact magnetically can be formed from the extra-framework iron as a result of heating and reaction with water vapor. Fe_{ext}-ZSM-5, which contains exchangeable Fe^{3+}, showed only the line at g ≈ 2, characteristic of Fe_xO_y clusters [15]. According to Tuan et al. [31], because the ionic radius of Fe^{3+} is larger than that of Si^{4+}, some extra-framework Fe can be formed. The line at g ≈ 4.7 is an indication that Fe^{3+} is present in the framework of the zeolites [33]. Using FTIR spectroscopy, Szostak et al. [33] also observed a band caused by framework Fe that appeared at 656 cm^{-1} (–(Si-O-Fe)n stretching). However, our FTIR spectra did not show a band at 656 cm^{-1}, nor any band characteristic of framework Fe. We also did not observe any band caused by iron oxide-hydroxides. An investigation in the region 25 cm^{-1} to 400 cm^{-1} was also performed; however, the spectra showed only characteristic bands of ZSM-5 zeolite. Joyner and Stockenhuber [13] and Ugrina et al. [20] also did not observe bands caused by

–(Si-O-Fe)n stretching or iron oxide-hydroxides. Another possibility is that the line at g ≈ 2 could be a result of iron cationic species {($Fe(H_2O)_6^{3+}$, $[Fe(H_2O)_5OH]^{2+}$, $[Fe(H_2O)_4(OH)_2]^{+}$, $Fe_2(OH)_2^{4+}$} adsorbed onto negatively charged zeolite surface [20]. According to them, at pH = 3.6, all those iron species could exist on a zeolite surface with $[Fe(H_2O)_5OH]^{2+}$ dominating. It should be noted that our experiments were performed at pH's in the range from 3.04 to 4.66 (Table 2). EPR spectra of samples of seawater 4.0 Ga mixed with zeolites showed a weak band at g ≈ 2, the spectrum of lyophilized seawater 4.0 Ga did not shown this band (Figure 5). Thus, a small amount of Fe^{3+} was withdrawn from the zeolites. Unlike X-ray diffraction methods, EPR is very sensitive: it can determine Fe^{3+} at levels of parts per billion (ppb). This confirms that seawater 4.0 Ga did not compromise the roles played by these zeolites.

Table 3 shows the values for each event for all zeolites tested without treatment and for lyophilized samples after the adsorption of adenine dissolved in seawater 4.0 Ga and ultrapure water. In the temperature range from 30 °C to 140 °C , with a maximum in the range 52 °C to 89 °C, all zeolites showed an event that it is characteristic of the loss of hydration water weakly bound to the zeolite [19, 60]. Zeolites mixed with seawater 4.0 Ga showed a higher loss of water than zeolites mixed with ultrapure water or without treatment (Table 3). This occurs because seawater 4.0 Ga contains divalent cations (Mg^{2+}, Ca^{2+}) which can be adsorbed onto the material surface, there being hydrated and water is retained on the zeolite [60, 64, 65]. Alver et al. [64] observed that dehydration is strongly dependent of the exchange cation and materials containing cations with high hydration energy, such as Ca^{2+}, contain significantly more H_2O than monovalent cations like K^{+}. It should be noted that

seawater 4.0 Ga is rich in Mg^{2+} and Ca^{2+} [30]. Besides Mg^{2+} and Ca^{2+} from seawater 4.0 Ga, more water was adsorbed into the cavities and surface of zeolites. This did not prevent the adsorption of adenine (Table 2).

Table 3 also shows a second event in the range from 140 °C to 360 °C, whose peaks ranged from 157 °C to 349 °C; some zeolites showed two peaks. This event could be caused by water strongly bound to exchangeable cations such as iron species or cations from seawater 4.0 Ga as well as from water located in the cavities of zeolites [19, 20, 60, 64]. The peaks of the second event showed two ranges of temperatures: one from 157 °C to 268 °C and other from 322 °C to 349 °C (Table 3). These ranges could be an indication that water is bound to different cations showing different dehydration enthalpies, probably Ca/Mg/Fe [60, 64, 66]. Mass loss for this event was much lower than that observed for the first event (Table 3). Other authors also observed a decrease in mass loss for the second event [60, 64]. The second event was not observed for two zeolites mixed with ultrapure water (Fe_7-ZSM-5, Fe_7-Adn-ZSM-5) and three with seawater 4.0 Ga (Fe_7-Adn-ZSM-5, Fe_{ext}-ZSM-5, Fe_{ext}-Adn-ZSM-5) (Table 3). Fe_7-Adn-ZSM-5 (ultrapure water, seawater 4.0 Ga) and Fe_{ext}-Adn-ZSM-5 adsorbed a high amount of adenine (Table 2). Thus, adenine could displace the water from the cations or the pores of zeolites and, consequently, the event was not observed.

All zeolites on which adenine was adsorbed showed an event between 360 °C and 600 °C (Figure 1 SM, Table 3). This event could be associated with thermal degradation of adenine that occurs in the temperature range from 247 °C to 438 ºC [67]. It should be noted that the mass loss (Table 3) follows almost the same order as the amount of adenine adsorbed onto zeolites (Table 2). For

zeolites without adenine adsorption, this event could be caused by the loss of more strongly associated water [19, 20, 60, 64].

The samples of the zeolite Fe_7-ZSM-5 with and without the treatments were subjected to XAFS analysis. Figure 6 shows the normalized XAFS spectra for the Fe_7-ZSM-5 zeolite samples. The pre-edge peak at 7114 eV could be attributed to quadrupole transitions from the 1s to 3d orbitals [68]. This transition is forbidden for octahedral coordination, but allowed for tetrahedral and distorted octahedral coordination [69]. This could be more evidence that Fe^{3+} was substituted into the framework of Fe_7-ZSM-5 zeolite, as was also shown by EPR spectroscopy (Figure 5-d). It should be noted that the sample Fe_7-ZSM-5-d (Figure 6-d) had an energy shift of the peak from 7114 eV to 7115 eV. This shift could be a result of interaction between Fe^{3+} and adenine. It should also be noted that, for the sample of adenine adsorbed onto Fe_7-ZSM-5-e (Figure 6-e) in seawater 4.0 Ga, this shift was not observed. This could mean that in ultrapure water adenine interacts with Fe^{3+} and in seawater 4.0 Ga adenine interacts with the cations adsorbed onto the zeolite. According to Battidtion et. al. [70], the shift of the pre-edge peak to higher energies was related to the decrease of symmetry and the coordination number of neighbors. The Fe_7-ZSM-5-d sample has a decrease of the coordination (CN) (Table 4) and the highest value of E_0 for all coordination shells. This behavior could be attributed to adsorption of adenine (Table 2, 4) its coordination to the Fe atom could promote a distortion in the symmetry and the energy shift on the pre-edge. FTIR spectra also showed an interaction between adenine and Fe_7-ZSM-5 zeolite (Figure 2-b).

Figure 7 shows the curves and the fitted spectra in χ(k) and the Fourier transform χ(R), all plotted with k^2-weighted spectra. The first peak, near 0.7 Å and 2.1 Å in in R-space, is due to the O shell around Fe in all five samples. For the sample Fe_7-ZSM-5-a, without previous treatment, the second peak at 2.1 Å to 2.9 Å is attributed to the Fe-Fe_1 shell. However, the samples Fe_7-ZSM-5-b, c, d, and e, with treatment (ultrapure water with and without adenine, seawater 4.0 Ga with and without adenine) showed a third peak at 2.9 Å to 3.4 Å that is attributed to the Fe-Fe_2 shell.

The parameters obtained from the fits to the multi-shell analysis are reported in table 4. The Fe_7-ZSM-5-a sample (without treatment) showed only two shells (Fe-O and Fe-Fe_1). The synthesis of an Fe-ZSM-5 resulted in the formation of a Fe_2O_3 clusters [71]. However, when the sample was submitted to any treatment (Fe_7-ZSM-5-b-e), it was transformed, and the best fit presented another Fe-Fe_2 shell. The second iron shell could be caused by the formation of hydroxide particles such as goethite (FeOOH) [72]. The distance for Fe-Fe_2 is 3.28 Å to 3.31 Å, which is close to the distance observed in goethite, which is 3.28 Å [73]. This could be explained by an interaction of the Fe with water (Fe_7-ZSM-5-b), cations of the seawater (Fe_7-ZSM-5-c), adenine (Fe_7-ZSM-5-d-e), or an association of all. It should be noted that EPR spectra showed a line at $g \approx 2$ that could be caused by Fe_xO_y clusters (Figure 5-d).

The decrease CN of the samples Fe_7-ZSM-5-c, d and e could be a result of the loss of Fe to the solution (e.g. by ion exchange), as it can be observed as a signal of g≈2 in the EPR spectroscopy (Figure 5-i), even if the X-ray diffractograms do not point to a dissolution of the material (Figure 4-e). Another explanation for the decrease is the formation of a hydroxide iron phase

as Goethite and hematite have a CN of 2 and 4 for the Fe-Fe_1 shell and 2 and 3 for the Fe-Fe_2 shell, respectively [72, 74].

The increase in the value of the E_0 of all shells, according to each treatment (Table 4), could be interpreted as an increase in the complexity of the system caused by the addition of the seawater and adenine and it could be concluded that the hematite reference is not enough to explain those systems (Fe_7-ZSM-5-d and e).

4. CONCLUSION

Adenine showed the highest adsorption onto Fe_{ext}-ZSM-5 (Fe^{+3} exchangeable), followed by Fe_7-ZSM-5. The adsorption of adenine was lower in Fe-ZSM-5 zeolites with iron isomorphically substituted. For Fe_7-ZSM-5 the adsorption was statistically different in ultrapure water and seawater 4.0 Ga. The pore size of zeolites had an effect on the adsorption of adenine.

FTIR spectra showed that the locus for interaction between the adenine and zeolite occurs at the adenine C=C and NH_2 groups.

The SEM images shows that Fe-ZSM-5 zeolite has spherical particles and the X-Ray diffractograms show that adenine had no effect on the dissolution of material. In treatments with seawater 4.0 Ga, the diffractograms showed precipitation of gypsum ($CaSO_4\,2H_2O$) onto zeolites.

EPR spectra of Fe_4-, Fe_6-, and Fe_7-ZSM-5 zeolites showed three lines: two in the region at $g \approx 2$ and another at $g \approx 4.7$. Fe_5-ZSM-5 showed one line at $g \approx 2$ and another at $g \approx 4.7$ and Fe_{ext}-ZSM-5 only one line at $g \approx 2$. The lines at $g \approx 2$ could be caused by Fe^{3+} species adsorbed onto zeolites as well as by the Fe framework. The line at $g \approx 4.7$ could be attributed to the Fe framework. FTIR

spectra did not show any characteristic band of framework Fe or any band caused by iron oxide-hydroxides.

TG curves for the zeolites showed an event between 30 °C and 140 °C, characteristic of the loss of hydration water weakly bound to the zeolite. The second event (140 °C to 360 °C) was a result of water bound to exchangeable iron species or cations from seawater 4.0 Ga and water located in the cavities of zeolites. Some zeolites showed two peaks (157 °C to 268 °C and 322 °C to 349 °C) in this region, probably because of the different dehydration enthalpies of the cations (Fe/Ca/Mg). The third event (360 °C to 600 °C) could be attributed to the degradation of adenine adsorbed onto zeolites and strongly associated water. For the zeolites with adenine adsorption, mass loss follows almost the same order as the amount of adenine adsorbed onto zeolites.

XAFS spectra of Fe_7-ZSM-5 zeolites showed a peak at 7114 eV, a transition that is allowed for tetrahedral or distorted octahedral coordination. This could be evidence that Fe^{3+} was substituted into the framework of Fe_7-ZSM-5 zeolite. After the adsorption of adenine onto Fe_7-ZSM-5 zeolite, a decrease in the CN and the highest value of E_0 for all coordination shells was observed. After the samples were submitted to treatments, a second iron shell was observed that could be a result of the formation of iron hydroxides. The increase in the value of the E_0 of all shells according to each treatment could be interpreted as an increase in the complexity of the system given by the addition of seawater 4.0 Ga and adenine, and it could be concluded that the hematite reference is not enough to explain those systems.

As general conclusion, this work shows the adsorption interaction between adenine and Fe-zeolite both coexisting in the prebiotic Earth. This

interaction is an issue of paramount importance for understanding prebiotic chemistry since adenine is key block for DNA synthesis and iron plays important roles in the biochemistry of today's living beings. In addition, despite iron being the fourth most abundant element in the Earth's crust, there are few studies into the possible roles played by this element in the origin of life. Finally, it should be noted that most experiments in prebiotic chemistry are performed under conditions that do not resemble the environment of prebiotic Earth. Using seawater 4.0 Ga the results obtained better resemble processes that could have happened in prebiotic Earth.

5. ACKNOWLEDGMENTS

PRA and JPTB acknowledge the PhD fellowships from CNPq and Capes, respectively. This research was supported by grants from Fundação Araucária (chamada 1, protocolo 23134), CNPq (474265/2013-7) and CNPq/Fundação Araucária (Programa de Apoio a Núcleos de Excelência – PRONEX, protocolo 24732). The use of XAFS1 beamline was supported by the Brazilian Synchroton Light Laboratory (LNLS/CNPEM) through proposal XAFS1-16161. C.C.C. thanks the Spanish MINECO for the "Ramón y Cajal" grant (RYC 2011-08550) at the Universidad de Cantabria. We acknowledge the use of the facilities of the Laboratorio de Microscopías Avanzadas at the Instituto de Nanociencia de Aragón, where the electron microscopy characterization was done, and the use of the Servicio General de Apoyo a la Investigación-SAI (Universidad de Zaragoza).

6. Author Disclosure Statement

On behalf of all authors, I guarantee that the present paper has not been published before, it is not presently being considered for publication elsewhere, it does not violate any intellectual property right of any person or entity, it does not contain any subject matter that contravenes any laws (including defamatory material and misleading and deceptive material), and it meets ethical standards applicable to the research discipline.

7. REFERENCES

[1] R.M. Hazen, D. Papineau, W. Bleeke, R.T. Downs, J.M. Ferry, T.J. McCoy, D.A. Sverjensky, H. Yang, Am. Mineral. 93 (2008) 1693–1720.

[2] R.L. Virta, Zeolites (natural). U.S. Geological Survey, Mineral Commodity Summaries, January 2011, U.S. Geological Survey, Reston, VA. Available online at http://minerals.usgs.gov/minerals/pubs/commodity/ zeolites/mcs-2011-zeoli.pdf, 2008.

[3] H.J. Cleaves, A.M. Scott, F.C. Hill, J. Leszczynsky, N. Sahai, R.M. Hazen, Chem. Soc. Rev. 41 (2012) 5502–5525.

[4] D.S. Coombs, A.J. Ellis, W. S.Fyfe, A.M. Taylor, Geochim. Cosmochim. Acta 17 (1959) 53–107.

[5] E.L. Shock, Orig. Life Evol. Biosph. 22 (1992) 67–102.

[6] F.A. Mumpton, Proc. Nat. Acad. Sci. USA 96 (1999) 3463–3470.

[7] E. Piera, M.A. Salomón, J. Coronas, M. Menéndez, J. Santamária, J. Membr. Sci. 149 (1998) 99–114.

[8] D. Papaioannou, P.D. Katsoulos, N. Panousis, H. Karatzias, Microp. Mesop. Mat. 84 (2005) 161-170.

[9] A.W. Burton, S.I. Zones, Introduction to zeolite Science and practice, 3º Ed, Elsevier, Richmond, 2007.

[10] M.M. Hatay, M.M. Oo, World Acad. Sci. Eng. Technol. 48 (2008) 114–120.

[11] S. Abelló, D. Montané, Chem. Sustainability 4 (2011) 1538–1556.

[12] P. Misaelides, Microp. Mesop. Mat. 144 (2011) 15–18.

[13] R. Joyner, M. Stockenhuber, J. Phys. Chem. B 103 (1999) 5963-5976.

[14] P. Fejes, K. Lázár, I. Marsi, A. Rockenbauer, L. Korecz, J.B. Nagy, S. Perathoner, G. Centi, Appl. Catal. A: General 252 (2003) 75–90.

[15] M.S. Kumar, M. Schwidder, W. Grüner, A. Brückner, J. Catal. 227 (2004) 384-397.

[16] R. Gonzalez-Olmos, U. Roland, H. Toufur, F.D. Kopinke, A.Georgi, Appl. Catal. B: Environ. 89 (2009) 356–364.

[17] R. Gonzalez-Olmos, F.D. Kopinke, K. Mackenzie, A.Georgi Environ. Sci. Technol. 47 (2013) 2353-2360.

[18] Y.C. Yaman, G. Gündüz, M. Dükkanci, Color. Technol. 129 (2012) 69-75.

[19] S.S. Masiero, N.R. Marcilio, O.W. Perez-Lopez, Catal. Letters 131 (2009) 194-202.

[20] M. Ugrina, N.M. Vukojević, A. Daković, Desalination Water Treatment 53 (2015) 3557-3569.

[21] I. Parsons, M.R. Lee, J.V. Smith, Proc. Nat. Acad. Sci. USA 95 (1998) 15173–15176.

[22] J.V. Smith, Proc. Nat. Acad. Sci. USA 95 (1998) 3370–3375.

[23] M. Schoonen, A. Smirnov, C.A Cohn, Ambio 33 (2004) 539-551.

[24] C.E.A. Carneiro, H. de Santana, C. Casado, J. Coronas, D.A.M. Zaia, Astrobiology 11 (2011) 409-418.

[25] J.P.T. Baú, C.E.A. Carneiro, I.G. de Souza Junior, C.M.D. de Souza, A.C.S. da Costa, E. di Mauro, C.T.B.V. Zaia, J. Coronas, C. Casado, H. de Santana, D.A.M. Zaia, Orig. Life Evol. Biosph. 42 (2012) 19-29.

[26] P.R. Anizelli, J.P.T. Baú, H.S. Nabeshima, M.F. da Costa, H. de Santana, D.A.M. Zaia, Spectrochim. Acta Part A 126 (2014) 184-192.

[27] E. Galli, G. Vezzalini, S. Quartieri, A. Alberti, Zeolites 19 (1997) 318-322.

[28] Z.A.D. Lethbridge, J.J. Williams, R.I. Walton, K.E. Evans, C.W. Smith, Microp. Mesop. Mat. 79 (2005) 339-352.

[29] D.A.M. Zaia, Amino Acids 27 (2004) 113–118.

[30] D.A.M. Zaia, Int. J. Astrobiol. 11 (2012) 229–234.

[31] V.A. Tuan, J.L. Falconer, R.D. Noble, Microp. Mesop. Mat. 41 (2000) 269-280.

[32] J. Kraczka, D.S. Kulgawczuk, A.Z. Hrynkiewicz, W. Zabiiqski, Hyperfine Interact. 29 (1986) 1129-1132.

[33] R. Szostak, V. Nair, T.L. Thomas, J. Chem. Soc., Faraday Trans. 1 83 (1987) 487-494.

[34] R. Roque-Malherbe, C. Díaz-Aguila, E. Reguera-Ruíz, J. Fundora-Lliteras, L. López-Colado, M. Hernández-Ruíz, Zeolites 10 (1990) 685-689.

[35] J.P. Ferris, W.J. Hagan Jr, Tetrahedron 40 (1984) 1093–1120.

[36] L.L. Hua, K. Kobayashi, E.I. Ochiai, C.W. Gehrke, K.O. Gerhardt, C. Ponnamperuma, Orig. Life Evol. Biosph. 16 (1986) 226–227.

[37] D.E. La Rowe, P. Regnier, Orig. Life Evol. Biosph. 38 (2008) 383–397.

[38] Z. Martins, O. Botta, M.L. Fogel, M.A. Sephton, D.P. Glavin, J.S. Watson, J.P. Dworkin, A.L. Schwartz, P. Ehrenfreund, Earth Planet. Sci. Lett. 270 (2008) 130–136.

[39] S.A. Wilde, J.W. Valley, W.H. Peck, C.M. Graham, Nature 409 (2001) 175-178.

[40] R.G. Strom, R. Malhotra, T. Ito, F. Yoshida, D.A. Kring, Science 309 (2005) 1847–1850.

[41] L.P. Knauth, Nature 395 (1998) 554–555.

[42] M.R.M. Izawa, H.W. Nesbitt, N.D. MacRae, E.L. Hoffman, Earth Planet. Sci. Lett. 298 (2010) 443–449.

[43] I. Melián-Cabrera, F. Kapteijn, J.A Moulijn, Catal. Today 110 (2005) 255–263.

[44] R.L. Blake, R.E. Hessevick, T. Zoltai, L.W. Finger, Am. Mineral. 51 (1966) 123-129.

[45] J.F. Lambert, Orig. Life Evol. Biosph. 38 (2008) 211–242.

[46] J.J. Christensen, J.H. Rytting, R.M. Izatt, Biochemistry 9 (1970) 4907-4913.

[47] G.E. Lailach, T.D. Thompson, G.W. Brindley, Clays Clay Miner. 16 (1968) 285–293.

[48] D. Winter, G. Zubay, Orig. Life Evol. Biosph. 25 (1995) 61–81.

[49] L. Perezgasga, A. Serrato-Díaz, A. Negrón-Mendonza, G.L. de Pablo, F.G. Mosqueira, Orig. Life Evol. Biosph. 35 (2005) 91–110.

[50] L.O.B. Benetoli, H. de Santana, C.T.B.V. Zaia, D.A.M. Zaia, Monatsh. Chem. 139 (2008) 753–761.

[51] A. Negrón-Mendoza, S. Ramos-Bernal, I.G. de Buen, IEEE Trans. Nuclear Sci. 57 (2010) 1223–1227.

[52] C.E.A. Carneiro, G. Berndt, I.G. de Souza Junior, C.M.D. de Souza, A. Paesano Jr, A.C.S. da Costa, E. di Mauro, H. de Santana, C.T.B.V. Zaia, D.A.M. Zaia, Orig. Life Evol. Biosph. 41 (2011) 453-468.

[53] H. J. Cleaves, C. M. Jonsson, C. L. Jonsson, D. A. Sverjensky, R. M. Hazen, *Astrobiology*, 10 (2010) 311-323.

[54] H. Hashizume, S. Van der Gaast, B. K. G. Theng, B.K.G. *Clays and Clay Minerals* 45 (2010) 469–475.

[55] C. A. Cohn, T. K. Hansson, H. S. Larson, S. J. Sowerby, N. H. Holm, *Astrobiology*, 1 (2001) 477-480.

[56] S. Munsch, M. Hartman, S. Ernst, Chem. Commun. (2001) 1978–1979.

[57] K. K. Gorshunova, A.H. Kanaan, O.S. Travkina, T.I.N. Pavlova, N.G. Grigoreva, M.L. Pavlov, B.I. Kutepov, Pet. Chem. 54 (2014) 132–136.

[58] R. Santamaria, E. Charro, A. Zacarías, M. Castro, J. Comput. Chem. 20 (1999) 511-530.

[59] T.A. Mohamed, I.A. Shabaan, W.M. Zoghaib, H. Husband, R.S. Farag, A.E.M.A. Alajhaz, J. Mol. Structure 938 (2009) 263-276.

[60] P. Castaldi, L. Santona, C. Cozza, V. Giuliano, C. Abbruzzese, V. Nastro, P. Melis, J. Mol. Structure 734 (2005) 99-105.

[61] Q. Chen, D.J. Frankel, N.V. Richardson, Langmuir 18 (2002) 3219–3225.

[62] T. Yamada, K. Shirasaka, A. Takano, M. Kawai, Surf. Sci. 561 (2004) 233–247.

[63] A. McNutt, S. Haq, R. Raval, Surf. Sci. 531 (2003) 131–144.

[64] B.E. Alver, M. Sakizci, E. Yörükoğullari, J. Therm. Anal. Calorim. 100 (2010) 19–26.

[65] P.R. Anizelli, J.P.T. Baú, F.P. Gomes, A.C.S. da Costa, C.E.A. Carneiro, C.T.B.V. Zaia, D.A.M. Zaia, Orig. Life Evol. Biosph. 45 (2015) 289-306.

[66] S.E. Rodriguez-Cruz, R.A. Jockusch, E.R. Williams, J. Am. Chem. Soc. 121 (1999) 8898–8906.

[67] M.S. Masoud, A. El-Merghany, A.M. Ramadan, M.Y. Abd El-Kaway, J. Therm. Anal. Calorim. 101 (2010) 839–847.

[68] M. Zhang, G. Pan, D. Zhao, G. He, Environ. Pollution 159 (2011) 3509-3514.

[69] E.J.M. Hensen, Q. Zhu, M.M.R.M. Hendrix, A.R. Overweg, P.J. Kooyman, M.V. Sychev, R.A. van Santen, J. Catal. 221 (2004) 560–574.

[70] A.A. Battiston, J.H. Bitter, W.M. Heijboer, F.M.F. de Groot, D.C. Koningsberger, J. Catal. 215 (2003) 279–293.

[71] P. Marturano, L. Drozdova, G.D. Pirngruber, A. Kogelbauer, R. Prins, Phys. Chem. Chem. Phys. 3 (2001) 5585-5595.

[72] A.A. Battiston, J.H. Bitter, F.M.F. de Groot, A.R. Overweg, O. Stephan, J.A. van Bokhoven, P.J. Kooyman, C. van der Spek, G. Vankó, D.C. Koningsberger, J. Catal. 213 (2003) 251–271.

[73] R.M. Cornell, Schwertmann U. The iron oxides. 2 ed. Darmstadt. Wiley-VCH, 2003.

[74] S. Suzuki, T. Suzuki, M. Kimura, Y. Takagi, K. Shinoda, K. Tohji, Y. Waseda, Appl. Surf. Sci. 169-170 (2001) 109-112.

Table 1. Fe-ZSM-5 zeolites preparation conditions. The Si/Fe gel composition was 100 for all the samples. The autoclave temperature was always 185ºC, as in Tuan et al. (2000). The amounts of each zeolite obtained in synthesis are in column 7.

Sample	Stirring		Volume gel (mL)	Autoclave time (h)	pH	Amount (g)	Si/Fe
	T (ºC)	Time (h)					
F_{ext}	25	2	50	-	1.1[a]	1.45	
F_3	25	1	35	72	-	0.32	10
F_4	25	24	70	48	10.75	0.45	4.6
F_5	25	24	70	48	-	0.50	5.3
F_6	60	24	70	48	-	0.44	10
F_7	60	24	70	48	-	0.34	18

[a] pH of the mixture after adding the parent ZSM-5 zeolite. The pH of the Fe aqueous solution had been set at 2.5.

Table 2: Amounts in μg of adenine adsorbed onto zeolites, BET surface and pore specific volume of material

ZSM-5	Si/Fe*	Ultrapure Water	pH**	***Seawater 4.0 Ga	pH**	S_{BET} (m^2/g)	V_p (cm^3/g)
Fe_{ext}	-	684 ± 2 ^{A}	3.07-4,20	663 ± 11 ^{A}	3.46-4.10	304 ± 4	0.20
Fe_7	18	265 ± 3 ^{aB}	4.13-4.64	236 ± 3 ^{bB}	4.54-4.68	325 ± 4	0.40

Fe_4	4.6	182 ± 5 ^{C}	4.08-4.20	177 ± 5 ^{C}	3.90-4.24	316 ± 5	0.18
Fe_5	5.3	120 ± 6 ^{D}	3.96-4.19	123 ± 4 ^{D}	3.82-4.06	333 ± 5	0.18
Fe_3	10.1	91 ± 7 ^{D}	4.03-4.06	84 ± 5 ^{E}	3.76-4.03	313 ± 5	0.16
Fe_6	10.4	50.9 ±7.2 ^{E}	4.07-4.66	40.5 ± 3.7 ^{F}	4.23-4.58	313 ± 5.1	0.18

The results of adsorption are presented as mean ± standard error of mean. The number of sets was five with one samples each set. It was added 720 μg of nucleic acid bases and 20 mg of zeolite. Fe_7-ZSM-5 (Si/Fe = 18.24); Fe_4-ZSM-5 (Si/Fe = 4.63); Fe_5-ZSM-5 (Si/Fe = 5.30); Fe_3-ZSM-5 (Si/Fe = 10.08); Fe_6-ZSM-5 (Si/Fe = 10.37) For the rows, averages with distinct lowercase letters are statistically different from each other by Tukey test ($p < 0.05$). For the columns, averages with distinct capital letters are statistically different from each other by Tukey test ($p < 0.05$). *Calculated by EDX. **Range of pH after 24h of stirring. ***Seawater was prepared as described by Zaia (2012).

Table 3: Loss of weight events from thermal analyses of zeolites without previous treatment, mixed with ultrapure water or seawater 4.0 Ga and distillated water plus adenine and artificial seawater 4.0 Ga plus adenine.

		1° Event (30-140)		2° Event (140-360 °C)		3° Event (360-600 ºC)		Total
	ZSM-5	Peak (°C)	% Loss	Peak (°C)	% Loss	Peak (°C)	% Loss	% Loss
Without treatment	Fe_3	60	5.9	322	1.2	477	1.2	8.3
	Fe_4	61	6.3	330	0.8	-	-	7.1
	Fe_5	62	4.6	256; 342	1.5; 0.7	-	-	6.8
	Fe_6	59	6.5	261; 336	0.9; 1.0	-	-	8.4
	Fe_7	68	4.5	228	2.0	-	-	6.5
	Fe_{ext}	74	6.5	226	1.0	414	2.2	9.7
	ZSM-5	Peak (°C)	% Loss	Peak (°C)	% Loss	Peak (°C)	% Loss	Total % Loss
	Fe_3	61	4.2	162; 327	1.4; 0.8	480	1.1	7.1

ultrapure water	Fe_3-Adn*	64	4.7	240; 334	0.5; 0.2	478	2.3	7.7
	Fe4	67	3.5	161; 349	1.8; 1.0	470	0.5	6.8
	Fe_4-Adn*	61	6.5	329	0.5	436	2.0	9.0
	Fe_5	61	4.3	157; 341	1.4; 1.5	472	0.8	8.0
	Fe_5-Adn*	58	6.1	329	0.5	446	1.4	8.1
	Fe_6	61	4.4	202; 343	1.4; 1.0	-	-	6.8
	Fe_6-Adn*	89	4.2	337	0.6	446	1.3	6.1
	Fe_7	62	3.0	-	-	-	-	3.0
	Fe_7-Adn*	84	2.9	-	-	467	3.4	6.3
	Fe_{ext}	71	6.9	238	1.7	391	1.4	10.0
	Fe_{ext}-Adn*	63	5.8	239	1.4	480	6.1	13.3
	ZSM-5	Peak (°C)	% Loss	Peak (°C)	% Loss	Peak (°C)	% Loss	Total % Loss
seawater 4.0 Ga	Fe_3	67	5.5	208; 340	1.4; 0.6	482	1.2	8.2
	Fe_3-Adn*	71	6.0	264	1.4	483	1.8	9.2
	Fe_4	52	5.2	257	1.5	-	-	6.7
	Fe_4-Adn*	74	8.7	268	1.1	451	1.5	11.3
	Fe_5	69	6.4	167; 339	2.3; 0.4	482	0.7	9.8
	Fe_5-Adn*	68	6.9	265	1.8	456	1.2	9.9
	Fe_6	70	8.4	210	1.8	-	-	10.2
	Fe_6-Adn*	74	10.3	270	2.3	441	1.2	13.8
	Fe_7	60	7.6	235	1.5	446	1.8	10.9
	Fe_7-Adn*	71	6.8	-	-	468	3.1	9.9
	Fe_{ext}	67	5.4	-	-	550	2.6	8.0
	Fe_{ext}-Adn*	69	9.5	-	-	482	5.4	14.9

Adn* = adenine adsorbed onto zeolite, Seawater 4.0 Ga was prepared as described by Zaia (2012). Fe_7-ZSM-5 (Si/Fe = 18.24); Fe_4-ZSM-5 (Si/Fe = 4.63); Fe_5-ZSM-5 (Si/Fe = 5.30); Fe_3-ZSM-5 (Si/Fe = 10.08); Fe_6-ZSM-5 (Si/Fe = 10.37)

Table 4: Fit parameters of multiple shell analysis of the EXAFS data for Fe_7-ZSM-5 samples.

Sample	Shell	**CN	ΔE_0 (eV)	R (Å)	σ (10^{-3} Å^2)
Fe_7-ZSM-5-a	O_1	2.6	-6.58	1.87	5
	Fe_1	2.6	-6.58	3.00	20
Fe_7-ZSM-5-b	O_1	3.0	-9.75	1.87	6
	*Fe_1	3.0	3.24	3.00	14
	*Fe_2	3.0	3.24	3.28	24
Fe_7-ZSM-5-c	O_1	2.9	-9.51	1.86	6
	*Fe_1	2.9	4.79	3.08	17
	*Fe_2	2.9	4.79	3.31	22
Fe_7-ZSM-5-d	O_1	2.6	-1.38	1.86	5
	*Fe_1	2.6	11.38	3.07	15
	*Fe_2	2.6	11.38	3.31	17
Fe_7-ZSM-5-e	O_1	2.5	-2.35	1.86	5
	*Fe_1	2.5	9.59	3.06	16
	*Fe_2	2.5	9.59	3.29	19

*Equal parameters of energy for Fe_1 and Fe_2 in each sample. **Equal parameters of amplitude for all shell in each sample. Fe_7-ZSM-5 (Si/Fe = 18.24) CN is the coordination number, ΔE_0 is the difference in energy between the sample and the reference compound, R is the atomic distance and σ is the Debye–Waller factor. **a)** without treatment; **b)** stirred with ultrapure water; **c)** stirred with seawater 4.0 Ga; **d)** stirred

with 720 µg mL^{-1} of adenine in ultrapure water; **e)** stirred with 720 µg mL^{-1} of adenine in seawater 4.0 Ga.

FIGURE CAPTIONS

Figure 1: Molecular structure of adenine

Figure 2: FTIR spectra: a_1) solid adenine; a_2) adenine adsorbed onto Fe_{ext}-ZSM-5 at pH 4.00 - ultrapure water; a_3) adenine adsorbed onto Fe_{ext}-ZSM-5 at pH 4.00 – seawater 4.0 Ga; a_4) solid $Fe_{ext;}$-ZSM-5 b_1) solid adenine; b_2) adenine adsorbed onto Fe_7-ZSM-5 at pH 4.00 - ultrapure water; b_3) adenine adsorbed onto Fe_7-ZSM-5 at pH 4.00 – seawater 4.0 Ga; b_4) solid Fe_7-ZSM-5; All samples were stirred for 24 h before being centrifuged for 5 min. at 6,000 rpm. The solid was separated from supernatant and lyophilized. The seawater 4.0 Ga was prepared as described by Zaia (2012).

Figure 3: SEM images from **a)** ZSM-5; **b)** Fe-ZSM-5 F_3 (Si/Fe=10); **c)** Fe-ZSM5 F_4 (Si/Fe=4.6); **d)** Fe-ZSM5 F_5 (Si/Fe=5.3); **e)** Fe-ZSM5 F_6 (Si/Fe=10); **f)** Fe-ZSM5 F_7 (Si/Fe=18). Scale: ZSM-5 = 5 μm; F_3 = 3 μm; F_4 = 3 μm; F_5 = 5 μm; F_6 = 5 μm; F_7 = 4 μm.

Figure 4: X-Ray diffraction patterns of Fe-ZSM-5 **a)** F_3; **b)** F_4; **c)** F_5; **d)** F_6; **e)** F_7 and f**)** F_{ext}, without treatment (----), after stirring in ultrapure water at pH 4.0 (----), after adsorption test of adenine in distillated water at pH 4.0 (----),after stirring in in seawater 4.0 Ga at pH 4.0 (----) and after adsorption test of adenine in seawater 4.0 Ga at pH 4.0 (----).

Figure 5: EPR spectra at 298 K a-e) of Fe-ZSM-5 zeolite without treatment (----), after adsorption test in seawater 4.0 Ga (----), after adsorption test in ultrapure water (----), f-j) of supernatant lyophilized after adsorption test in seawater 4.0 Ga and k) seawater 4.0 Ga lyophilized. The seawater 4.0 Ga was prepared as described by Zaia (2012).

Figure 6: Normalized Fe K-edge XAFS for the samples Fe_7-ZSM-5 a-e: **a)** without treatment; **b)** stirred with ultrapure water; **c)** stirred with seawater 4.0 Ga; **d)** stirred with 720 μg mL^{-1} of adenine in ultrapure water; **e)** stirred with 720 μg mL^{-1} of adenine in seawater 4.0 Ga.

Figure 7: EXAFS (line) spectra and (dot) fit of the samples Fe_7-ZSM-5: **a)** without treatment; **b)** stirred with ultrapure water; **c)** stirred with seawater 4.0 Ga; **d)** stirred with 720 μg mL^{-1} of adenine in ultrapure water; **e)** stirred with 720 μg mL^{-1} of adenine in seawater 4.0 Ga.

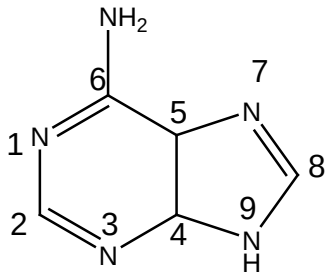

Adenine

Figure 1: Molecular structure of adenine

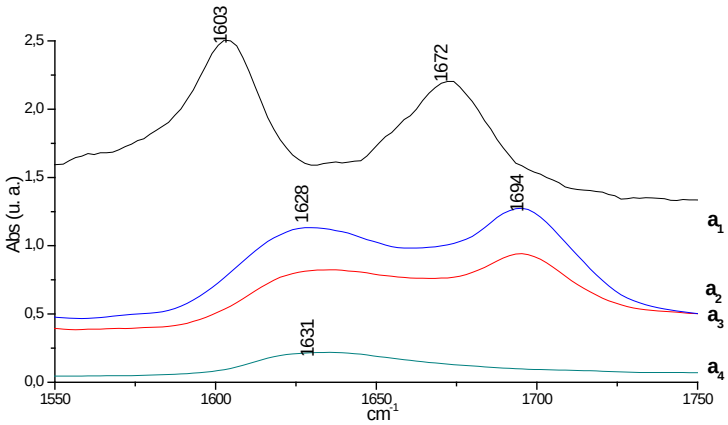

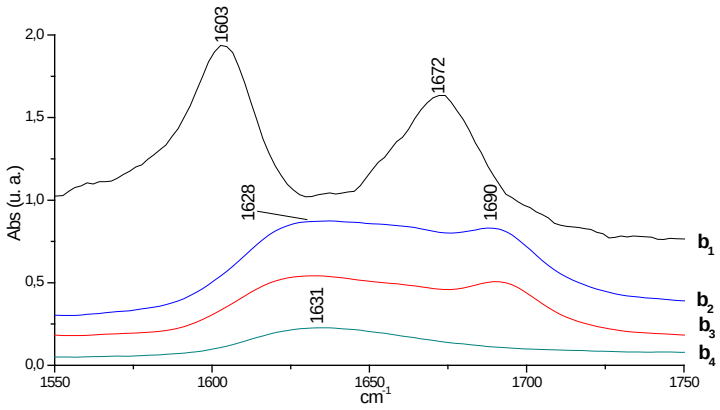

Figure 2: FTIR spectra: a_1) solid adenine; a_2) adenine adsorbed onto Fe_{ext}-ZSM-5 at pH 4.00 - ultrapure water; a_3) adenine adsorbed onto Fe_{ext}-ZSM-5 at pH 4.00 – seawater 4.0 Ga; a_4) solid $Fe_{ext;}$-ZSM-5 b_1) solid adenine; b_2) adenine adsorbed onto Fe_7-ZSM-5 at pH 4.00 - ultrapure water; b_3) adenine adsorbed onto Fe_7-ZSM-5 at pH 4.00 – seawater 4.0 Ga; b_4) solid Fe_7-ZSM-5; All samples were stirred for 24 h before being centrifuged for 5 min. at 6,000 rpm. The solid was separated from supernatant and lyophilized. The seawater 4.0 Ga was prepared as described by Zaia (2012).

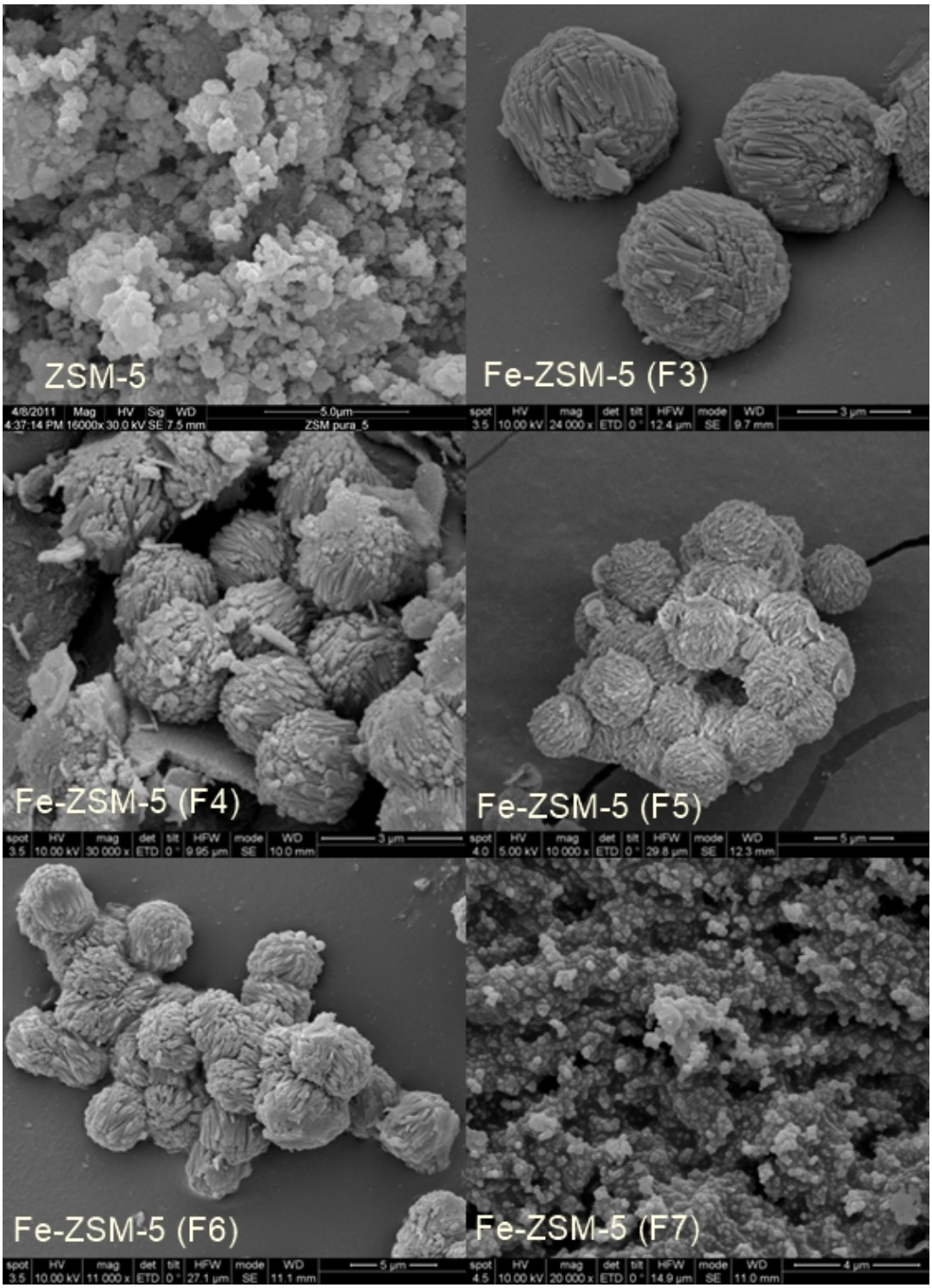

Figure 3: SEM images from **a)** ZSM-5; **b)** Fe-ZSM-5 F_3 (Si/Fe=10); **c)** Fe-ZSM5 F_4 (Si/Fe=4.6); **d)** Fe-ZSM5 F_5 (Si/Fe=5.3); **e)** Fe-ZSM5 F_6 (Si/Fe=10); **f)** Fe-ZSM5 F_7 (Si/Fe=18). Scale: ZSM-5 = 5 μm; F_3 = 3 μm; F_4 = 3 μm; F_5 = 5 μm; F_6 = 5 μm; F_7 = 4 μm.

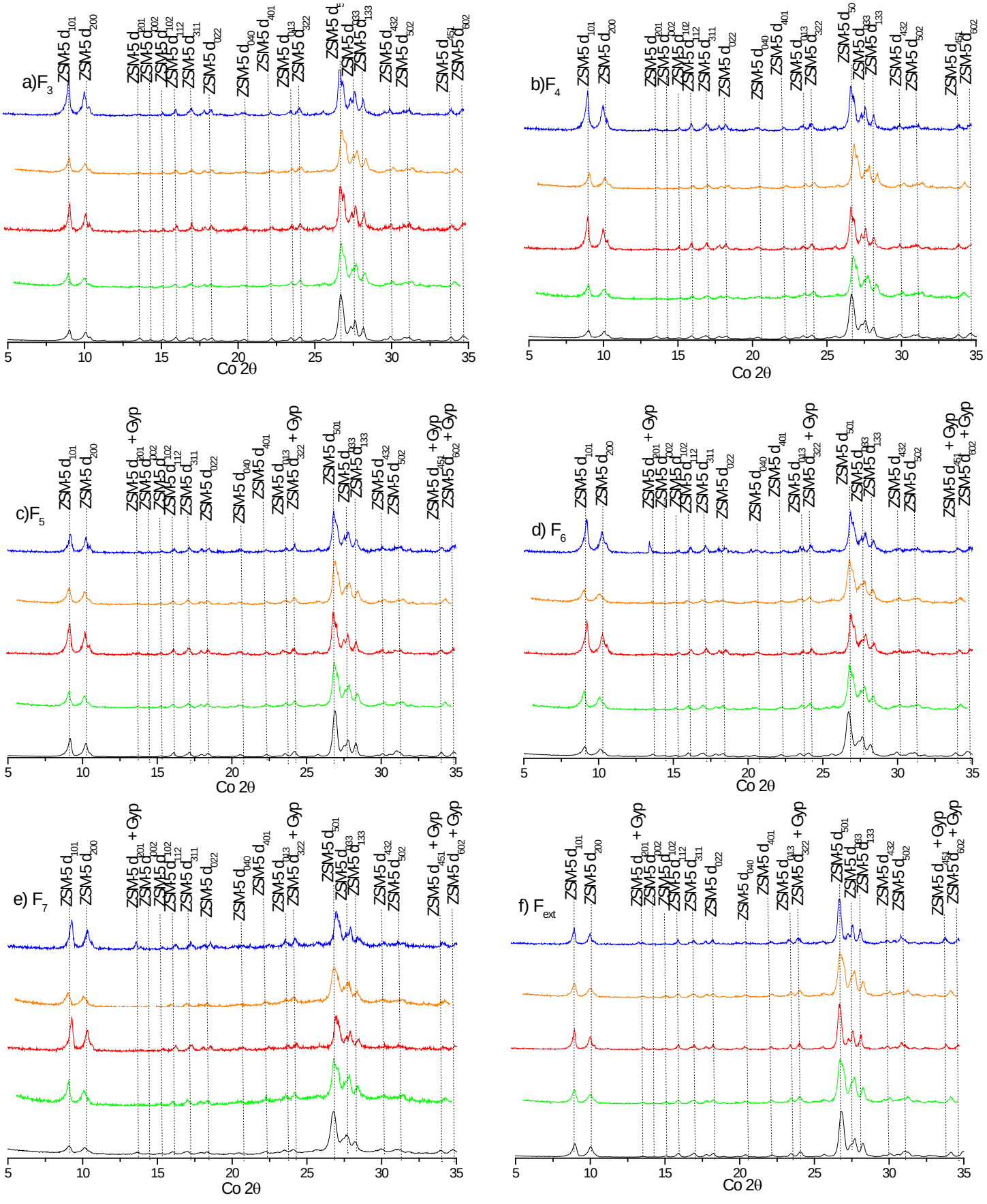
a)F3
b)F4
c)F5
d) F6
e) F7
f) Fext
ZSM-5 d101
ZSM-5 d200
ZSM-5 d201
ZSM-5 d002
ZSM-5 d102
ZSM-5 d112
ZSM-5 d311
ZSM-5 d022
ZSM-5 d040
ZSM-5 d401
ZSM-5 d013
ZSM-5 d322
ZSM-5 d501
ZSM-5 d133
ZSM-5 d432
ZSM-5 d502
ZSM-5 d451
ZSM-5 d602
+ Gyp
Co 2θ
5
10
15
20
25
30
35

Figure 4: X-Ray diffraction patterns of Fe-ZSM-5 **a)** F_3; **b)** F_4; **c)** F_5; **d)** F_6; **e)** F_7 and f) F_{ext}, without treatment (----), after stirring in ultrapure water at pH 4.0 (----), after adsorption test of adenine in distillated water at pH 4.0 (----),after stirring in in seawater 4.0 Ga at pH 4.0 (----) and after adsorption test of adenine in seawater 4.0 Ga at pH 4.0 (----).

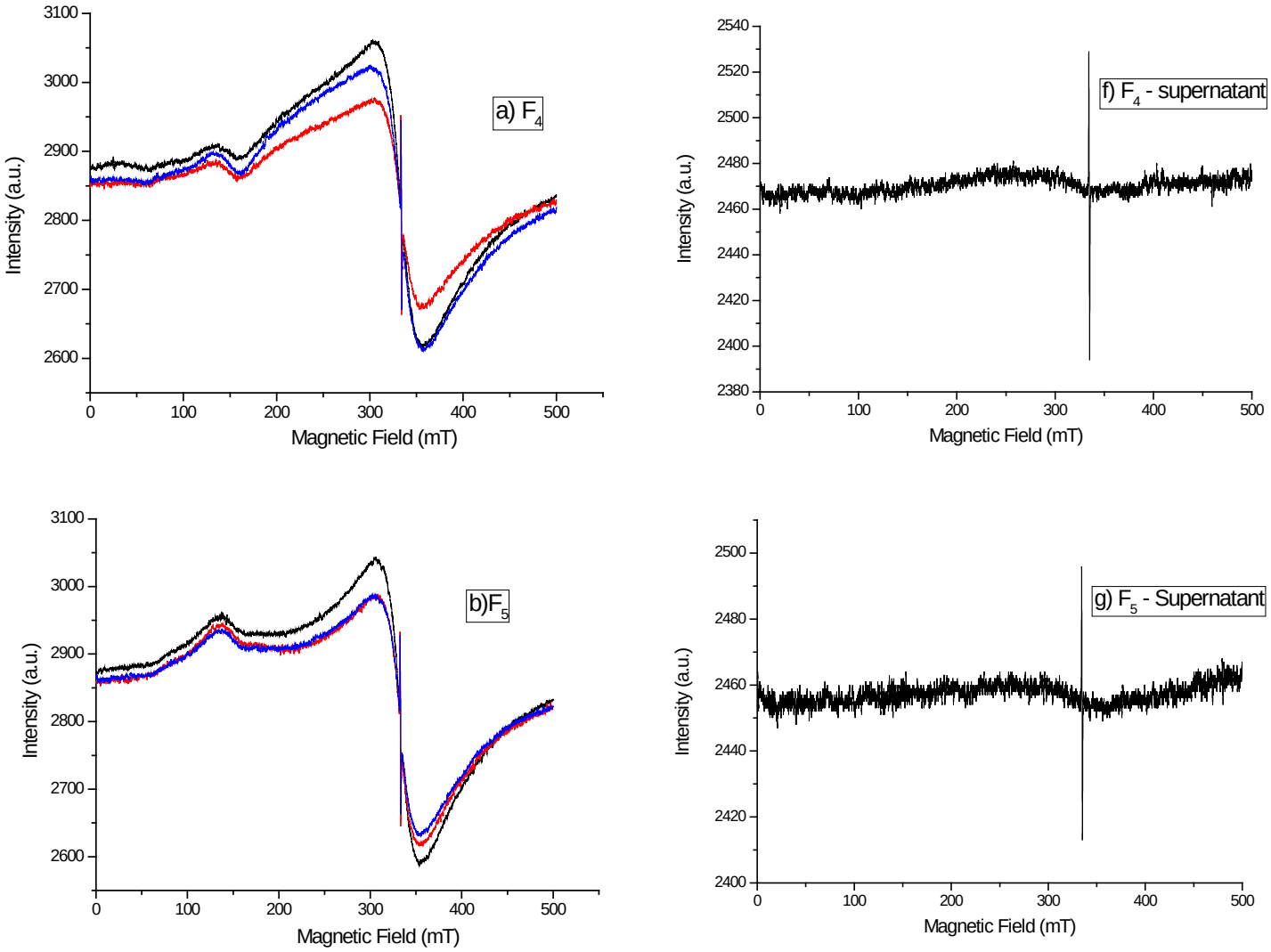

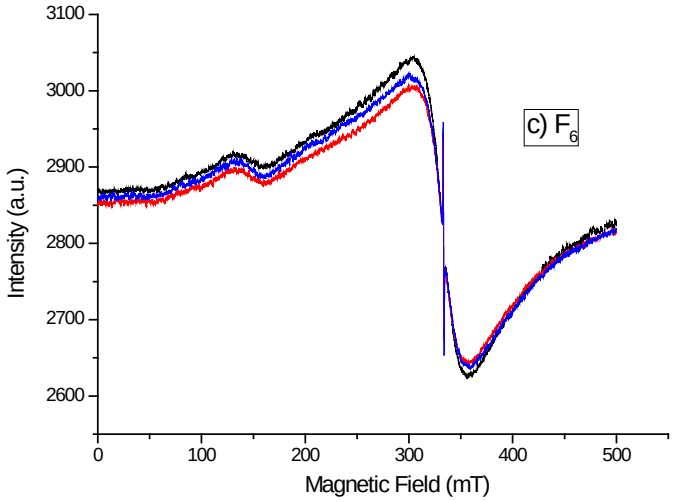
c) F6
Intensity (a.u.)
Magnetic Field (mT)

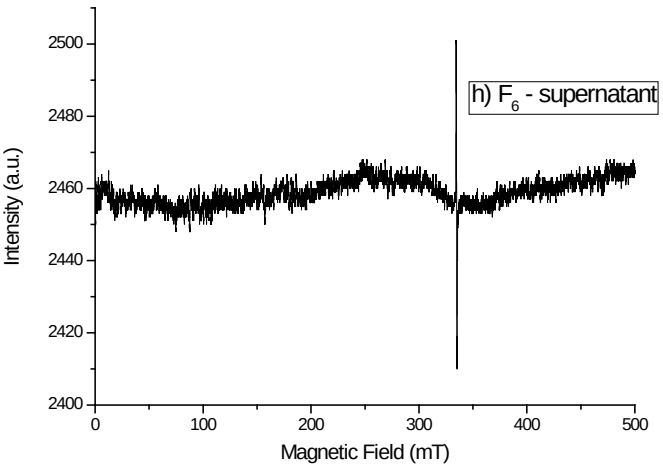
h) F6 - supernatant
Intensity (a.u.)
Magnetic Field (mT)

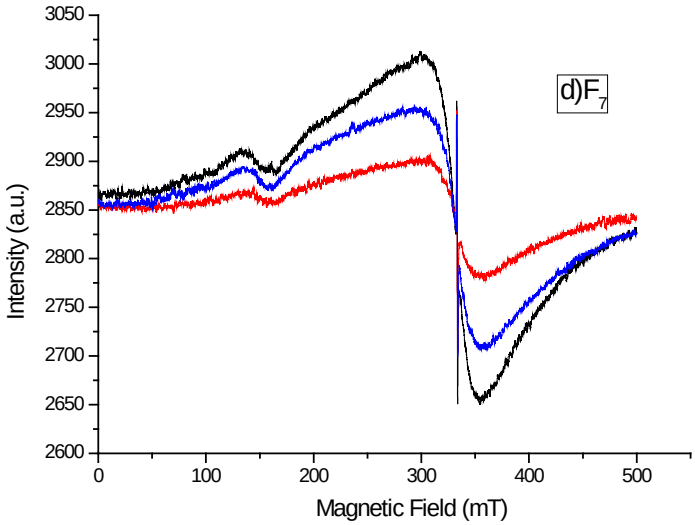
d)F7
Intensity (a.u.)
Magnetic Field (mT)

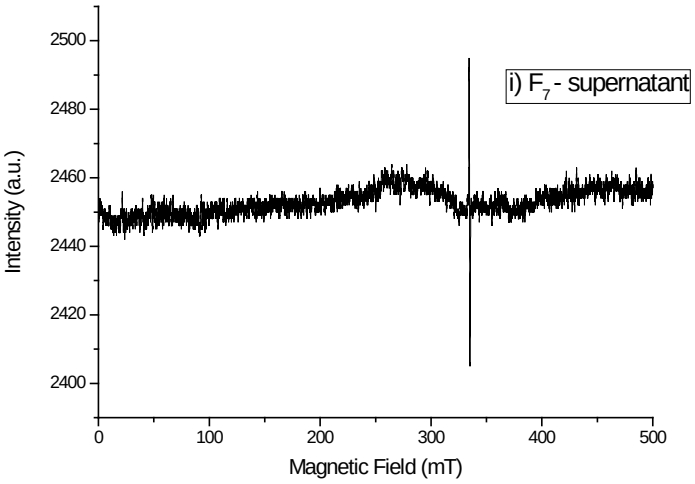
i) F7 - supernatant
Intensity (a.u.)
Magnetic Field (mT)

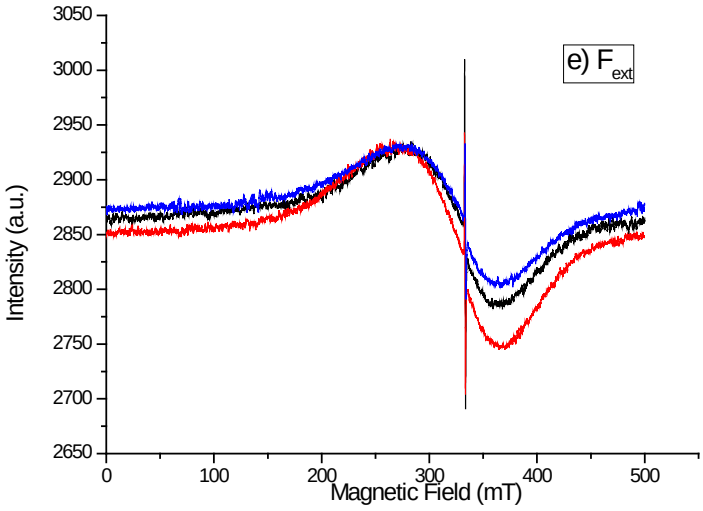
e) Fext
Intensity (a.u.)
Magnetic Field (mT)

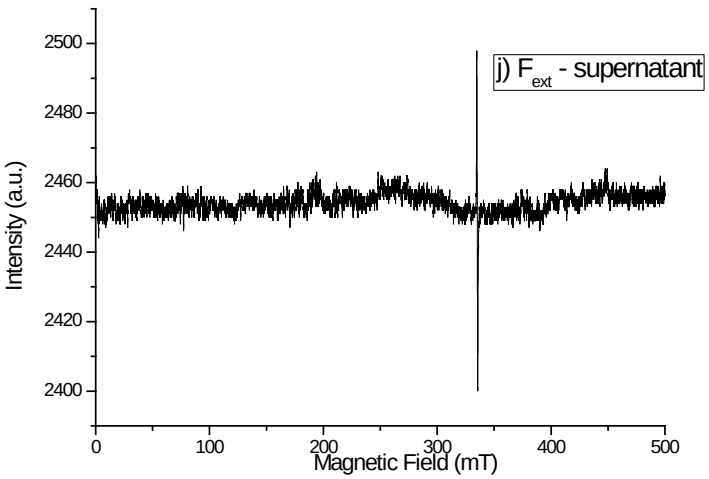
j) Fext - supernatant
Intensity (a.u.)
Magnetic Field (mT)

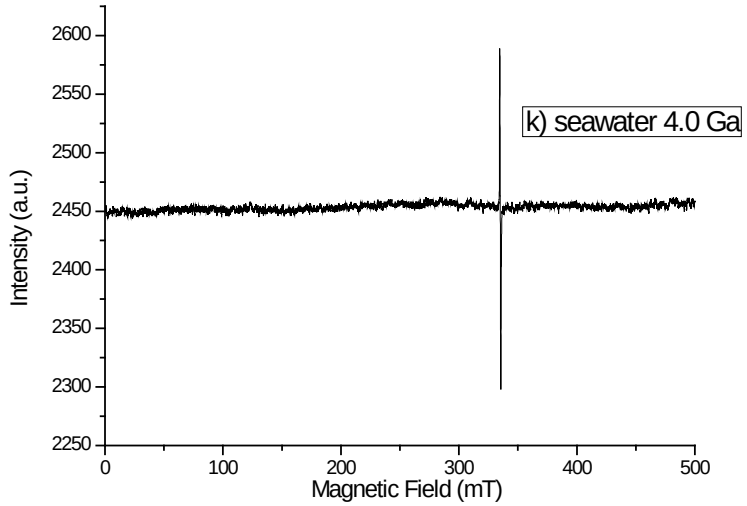

Figure 5: EPR spectra at 298 K a-e) of Fe-ZSM-5 zeolite without treatment (----), after adsorption test in seawater 4.0 Ga (----), after adsorption test in ultrapure water (----), f-j) of supernatant lyophilized after adsorption test in seawater 4.0 Ga and k) seawater 4.0 Ga lyophilized. The seawater 4.0 Ga was prepared as described by Zaia (2012).

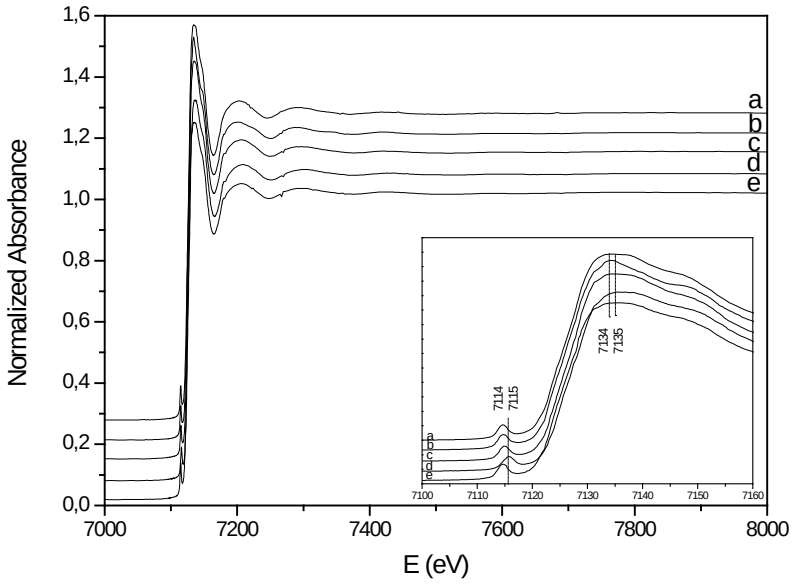

Figure 6: Normalized Fe K-edge XAFS for the samples Fe_7-ZSM-5 a-e: **a)** without treatment; **b)** stirred with ultrapure water; **c)** stirred with seawater 4.0 Ga; **d)** stirred with 720 μg mL^{-1} of adenine in ultrapure water; **e)** stirred with 720 μg mL^{-1} of adenine in seawater 4.0 Ga.

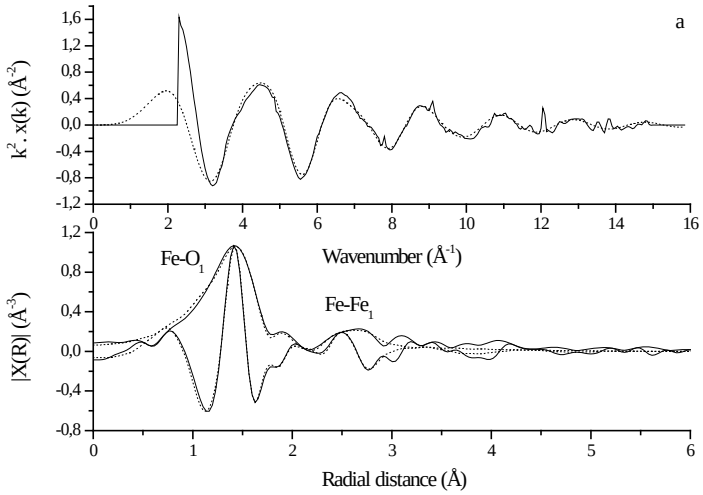
a
k². x(k) (Å⁻²)
Wavenumber (Å⁻¹)
Fe-O1
Fe-Fe1
|X(R)| (Å⁻³)
Radial distance (Å)

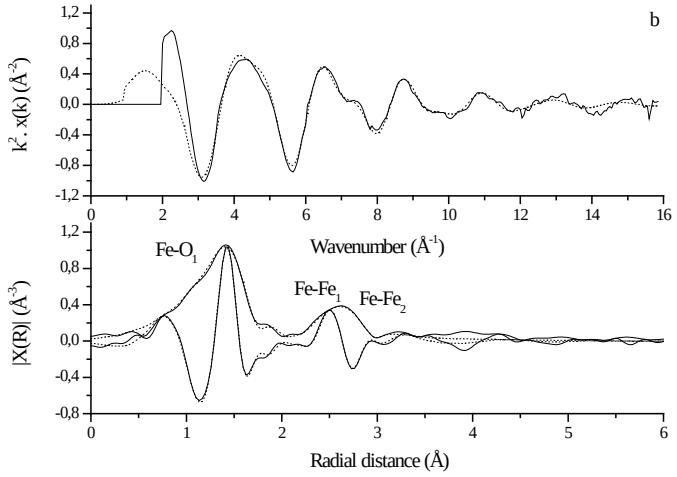
b
k². x(k) (Å⁻²)
Wavenumber (Å⁻¹)
Fe-O1
Fe-Fe1
Fe-Fe2
|X(R)| (Å⁻³)
Radial distance (Å)

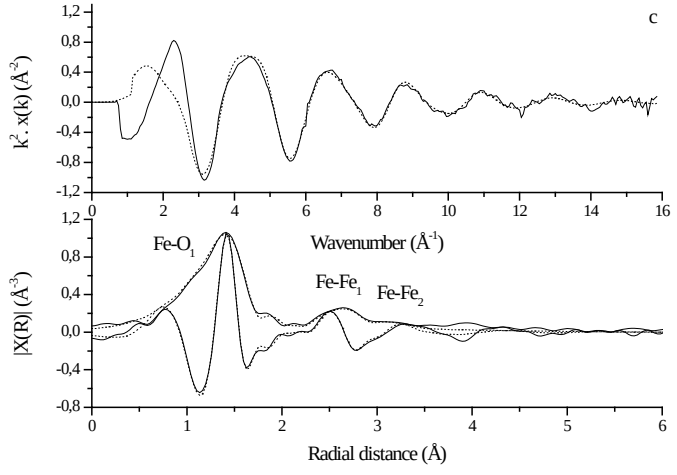
c
k². x(k) (Å⁻²)
Wavenumber (Å⁻¹)
Fe-O1
Fe-Fe1
Fe-Fe2
|X(R)| (Å⁻³)
Radial distance (Å)

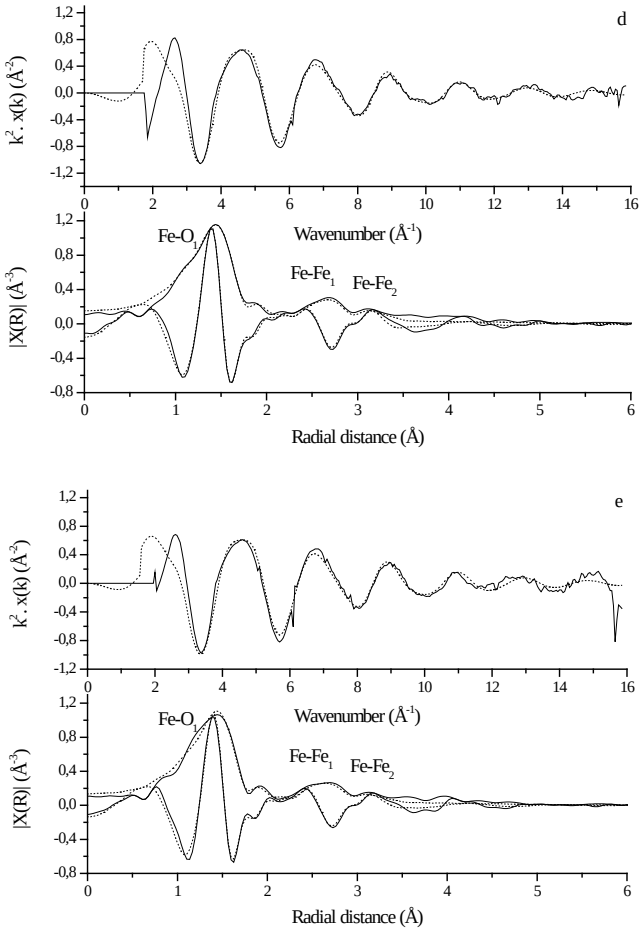

Figure 7: EXAFS (line) spectra and (dot) fit of the samples Fe_7-ZSM-5: **a)** without treatment; **b)** stirred with ultrapure water; **c)** stirred with seawater 4.0 Ga; **d)** stirred with 720 μg mL^{-1} of adenine in ultrapure water; **e)** stirred with 720 μg mL^{-1} of adenine in seawater 4.0 Ga.